Diagn Interv Radiol 2026; DOI: 10.4274/dir.2026.263750

CARDIOVASCULAR IMAGING

ORIGINAL ARTICLE

©Copyright 2026 Author(s) - Available online at dirjournal.org.
Content of this journal is licensed under a Creative Commons Attribution-NonCommercial 4.0 International License.

Magnetic resonance imaging evaluation of myocardial and hepatic tissue remodeling and cardiac function in sickle cell anemia

Serhat Başaran
Kaan Esen
Aydan Akdeniz
Hasan H. Yüksek
Yüksel Balcı

Mersin University, Department of Radiology, Mersin, Türkiye

PURPOSE

To assess myocardial and hepatic tissue remodeling in patients with sickle cell anemia (SCA) using T1 mapping and extracellular volume (ECV) measurements, and to evaluate diastolic dysfunction (DD) using magnetic resonance imaging (MRI).

METHODS

This prospective study enrolled 32 patients with SCA (19 women; mean age: 37 years) and 12 healthy controls (8 men; mean age: 31 years). Myocardial T1, T2, and T2* values and hepatic T1 and T2* values were measured in both groups. Myocardial and hepatic ECV measurements were performed in the patient group. DD was evaluated using transmitral flow (TMF) curves and left atrial volume index (LAVI).

RESULTS

In patients with SCA, the mean myocardial T1 value was 1,030.91 ms, significantly higher than in controls, and the mean ECV was 31.7% ± 3.1%, higher than published reference ranges. Moreover, LAVI was significantly higher in patients than in controls (46.48 ± 15.35 vs. 30.58 ± 5.0 mL/m^2; $P < 0.001$). Diastolic function assessment revealed findings suggestive of a restrictive filling pattern in 10 individuals, who had an average age of 33 years. Within the SCA cohort, patients with TMF-derived early/late ratio >2 (n = 10) had significantly higher LAVI than the remaining patients (54.05 ± 10.12 vs. 43.0 ± 16.26 mL/m^2; $P = 0.027$). Myocardial ECV was significantly higher in patients with findings suggestive of a restrictive filling pattern than in the remaining patients (34.14% ± 2.39% vs. 30.62% ± 2.67%; $P = 0.001$). The mean myocardial T2* value was 39.25 ± 5.9 ms, and no cardiac iron accumulation was detected. The mean hepatic T2* value was 12.20 ms, with iron accumulation observed in 16 patients. Iron accumulation can have an impact on T1 values, and measurements in patients without iron accumulation revealed a mean liver T1 value (626.5 ms) that was significantly higher than that in controls ($P < 0.001$). These patients also had an ECV (40.4%) that was higher than published reference ranges ($P < 0.001$).

CONCLUSION

Increased myocardial and hepatic T1 and ECV values were observed in patients with SCA, suggesting expansion of the extracellular space, largely consistent with diffuse interstitial fibrosis in this clinical context. Diastolic function assessment revealed a restrictive filling pattern in a substantial proportion of patients, supporting a possible association between SCA and this pattern. Myocardial ECV was significantly higher in patients with findings suggestive of a restrictive filling pattern than in the remaining patients, suggesting an association between diffuse interstitial fibrosis and advanced DD patterns. MRI may be a valuable modality for evaluating myocardial and hepatic fibrosis and assessing cardiac function.

CLINICAL SIGNIFICANCE

MRI with mapping and ECV quantification may contribute to a non-invasive, quantitative assessment of myocardial and hepatic fibrosis-related tissue remodeling in patients with SCA. Moreover, TMF analysis may provide valuable insights into diastolic function. Together, these methods could contribute to the clinical evaluation and management of SCA and other diseases characterized by fibrosis-related remodeling.

KEYWORDS

Myocardial fibrosis, hepatic fibrosis, T1 mapping, extracellular volume, sickle cell anemia, cardiac function, diastolic dysfunction, T2* mapping

Handling editor: Furkan Ufuk

Corresponding author: Serhat Başaran

E-mail: serhat_4432@hotmail.com

Received 17 November 2025; revision requested 15 December 2025; last revision requested 10 February 2026; accepted 24 February 2026.

Epub: 18.03.2026

Publication date: 02.11.2026

DOI: 10.4274/dir.2026.263750

You may cite this article as: Başaran S, Esen K, Akdeniz A, Yüksek HH, Balcı Y. Magnetic resonance imaging evaluation of myocardial and hepatic tissue remodeling and cardiac function in sickle cell anemia. *Diagn Interv Radiol*. 2026;32(6):777-786.

Sickle cell anemia (SCA) is an autosomal recessive genetic disorder characterized by erythrocytes containing abnormal hemoglobin that become spherical and rigid under the influence of various stressors in the vascular microenvironment. Chronic hemolysis and recurrent ischemia-reperfusion injury in multiple organs constitute the fundamental mechanisms underlying the disease.[1] SCA-associated cardiac disease is one of the leading causes of mortality and morbidity in young adults.[2] Repeated microvascular occlusions result in ischemia and myocardial fibrosis. Additionally, chronic inflammation contributes to these processes, thereby impairing diastolic function. Diastolic dysfunction (DD), classified as impaired relaxation, pseudonormal, or restrictive filling patterns, is an independent risk factor for mortality.[3] Similarly, hepatic complications are frequently encountered and represent a significant cause of morbidity, negatively affecting prognosis. Processes such as ischemia and sequestration caused by vaso-occlusion, as well as iron accumulation from chronic hemolysis or treatment, can result in hepatic fibrosis.[4]

Cardiovascular magnetic resonance (CMR) imaging provides a comprehensive, non-invasive assessment of cardiac morphology and function, is highly reproducible, and plays a central role in myocardial tissue characterization using multiparametric techniques. Cine CMR provides high-temporal-resolution assessment of left ventricle and right ventricle function and enables accurate, highly reproducible three-dimensional quantification of ventricular volumes and ejection fraction (EF) without geometric assumptions. Phase-contrast (PC)-CMR can quantify blood-flow velocity and flow across vessels and heart valves, including transmitral flow (TMF) and pulmonary venous flow.[5] Late gadolinium enhancement (LGE) is widely used for detecting focal replacement fibrosis/scarring.[6] However, LGE may be limited in diffuse interstitial processes, making parametric mapping techniques increasingly important. Native T1 mapping and post-contrast extracellular volume (ECV) quantification enable detection and quantification of diffuse myocardial fibrosis, whereas T2 mapping can provide complementary information related to edema/inflammation.[7] In addition, T2* mapping is an established quantitative approach for assessing myocardial iron deposition in transfusion-related iron overload and other iron storage conditions.[8] For the liver, magnetic resonance imaging (MRI) relaxometry-based approaches (including R2/R2* and T2*) are increasingly used for non-invasive quantification of liver iron concentration and longitudinal follow-up, enabling assessment of transfusional iron burden alongside fibrotic remodeling.[9] Moreover, liver T1 mapping and ECV measurements have been explored as non-invasive markers of hepatic fibrosis and have been shown to correlate with fibrosis severity in chronic liver disease.[10]

The primary aim of this study was to evaluate myocardial fibrosis in patients with SCA using MRI-based T1 mapping and ECV measurements. DD, which may be related to fibrotic remodeling, was assessed using TMF analysis and left atrial (LA) volume index (LAVI) measurements. Hepatic tissue characterization was performed in parallel with myocardial assessment; T2* mapping was also performed to assess myocardial and hepatic iron deposition that could confound fibrosis-related metrics.

Main points

- Magnetic resonance imaging can contribute to the non-invasive assessment of fibrosis-related tissue remodeling through mapping techniques and provide insight into diastolic function using transmitral flow (TMF) analysis.
- In patients with sickle cell anemia (SCA), increased myocardial and hepatic native T1 and extracellular volume values may indicate the presence of fibrosis.
- Diastolic function evaluation using TMF curves and left atrial volume analysis revealed that findings suggestive of restrictive filling patterns were relatively common among patients with SCA, suggesting a potential association.

Methods

Study design and participants

In this prospective study, cardiac and hepatic MRI examinations were performed on 32 patients with SCA (19 women, 13 men; mean age: 37 years) and 12 healthy controls (4 women, 8 men; mean age: 31 years) between September 2022 and March 2023. This study was approved by the Mersin University Clinical Research Ethics Committee (approval date: June 22, 2022; decision number: 2022/430). Written informed consent was obtained from all participants prior to inclusion in the study. Exclusion criteria included valvular heart disease, implanted cardiac devices, myocardial infarction, contrast allergies, diabetes, hypertension, cardiotoxic drug use, renal failure, pregnancy, age under 18 years, or refusal to provide informed consent. Blood samples were collected to assess hematocrit levels for ECV measurements. The flow of participant recruitment and exclusion is shown in Figure 1.

Magnetic resonance imaging technique

The MRI protocol included myocardial T1, T2, and T2* mapping and hepatic T1 and T2* mapping, in both the patient group and the control group. Myocardial and hepatic ECV measurements were performed, and LAVI and TMF curves were obtained to assess diastolic function in both groups. All examinations were performed using a 1.5-Tesla (T) MRI scanner (MAGNETOM Aera, Siemens Healthineers, Erlangen, Germany).

Native T1 mapping images of the heart and liver were acquired before contrast administration using the MOLLI sequence [parameters for cardiac imaging: repetition time

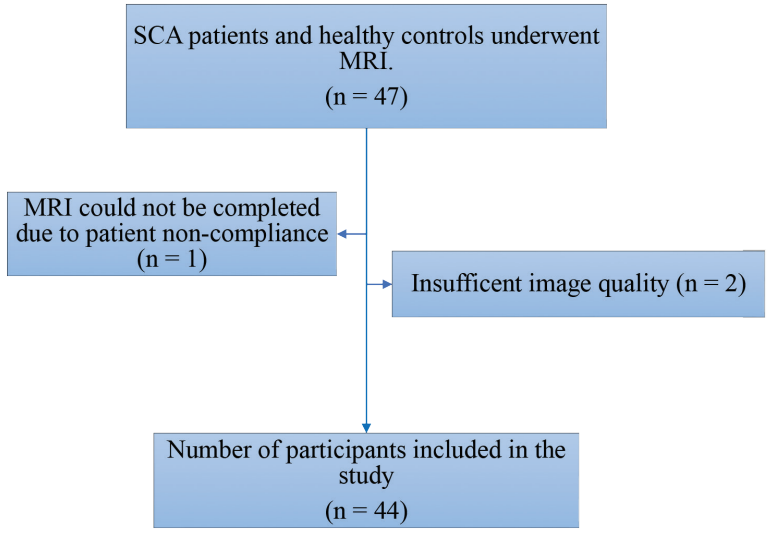


Figure 1. Flow diagram of the study. SCA, sickle cell anemia; MRI, magnetic resonance imaging.

(TR): 280.5 ms; time to echo (TE): 1.12 ms; flip angle: 35°; voxel size: 1.4 × 1.4 × 8.0 mm^3; for liver imaging: TR: 362.16 ms; TE: 1.12 ms; flip angle: 35°; voxel size: 1.4 × 1.4 × 8.0 mm^3]. After acquiring the native T1 maps, a contrast agent was administered intravenously at a dose of approximately 0.10 mmol/kg (gadobutrol, Gadovist®, Bayer AG, Berlin, Germany). Contrast-enhanced T1 mapping images were obtained 10–15 minutes later.

To evaluate hepatic and cardiac iron deposition, T2* maps were obtained before contrast administration using a multi-echo gradient-echo sequence with eight echo times (TE: 1.2, 3, 5, 7, 9, 11, 13, and 15 ms). TMF assessment was performed using PC-MRI. The imaging plane was planned on four-chamber cine images and was prescribed to be parallel to the mitral annulus at the level of the mitral valve leaflet tips at end-diastole. The resulting PC acquisition corresponds anatomically to a short-axis orientation at the level of the mitral valve. A through-plane velocity encoding value of 150 cm/s was used, and it was adjusted as needed to avoid velocity aliasing.

Magnetic resonance imaging analysis

Image analysis was conducted with the vendor-provided syngo.via post-processing software.

Myocardial native T1 times were calculated on pre-contrast T1 mapping images by drawing regions of interest (ROIs) on the left ventricular myocardium at the mid-ventricular level. A global myocardial approach was used, with ROIs encompassing most of the left ventricular wall while excluding the blood pool, papillary muscles, and trabeculations to minimize partial-volume effects.

Hepatic native T1 times were measured on pre-contrast T1 mapping images by placing a single, conservatively sized, circular-to-oval ROI in a homogeneous area of the right hepatic lobe. Measurements were performed once per patient using a representative slice. The ROI was positioned at least 1 cm away from the liver capsule, and areas affected by vascular structures, bile ducts, focal lesions, or susceptibility-related artifacts were visually identified and excluded to minimize partial-volume effects, using the same ROI template across patients. Considering the T1-shortening effect of iron deposition,[11,12] hepatic T1 values were calculated and analyzed both in the entire patient cohort and separately in patients without hepatic iron overload.

Myocardial and hepatic ECV values were calculated using post-contrast T1 values obtained by drawing corresponding ROIs on post-contrast T1 mapping images for both the myocardium and liver. Blood-pool T1 values were acquired from the left ventricular cavity and abdominal aorta on both pre- and post-contrast images (Figure 2). On the same day, the patient's blood hematocrit level was measured, and ECV values were calculated using the following formula:

$$ECV = (1\text{-}hematocrit) \times \left(\frac{1/T1(myo/liver\ postcontrast) - 1/T1(myo/liver\ precontrast)}{1/T1(blood\ postcontrast) - 1/T1(blood\ precontrast)}\right).$$

Myocardial T2* measurement was performed by manually drawing an ROI in the interventricular septum at the mid-ventricular level (Figure 3). A conservative, oval-to-circular ROI of standardized size was used to minimize partial-volume effects. The ROI was

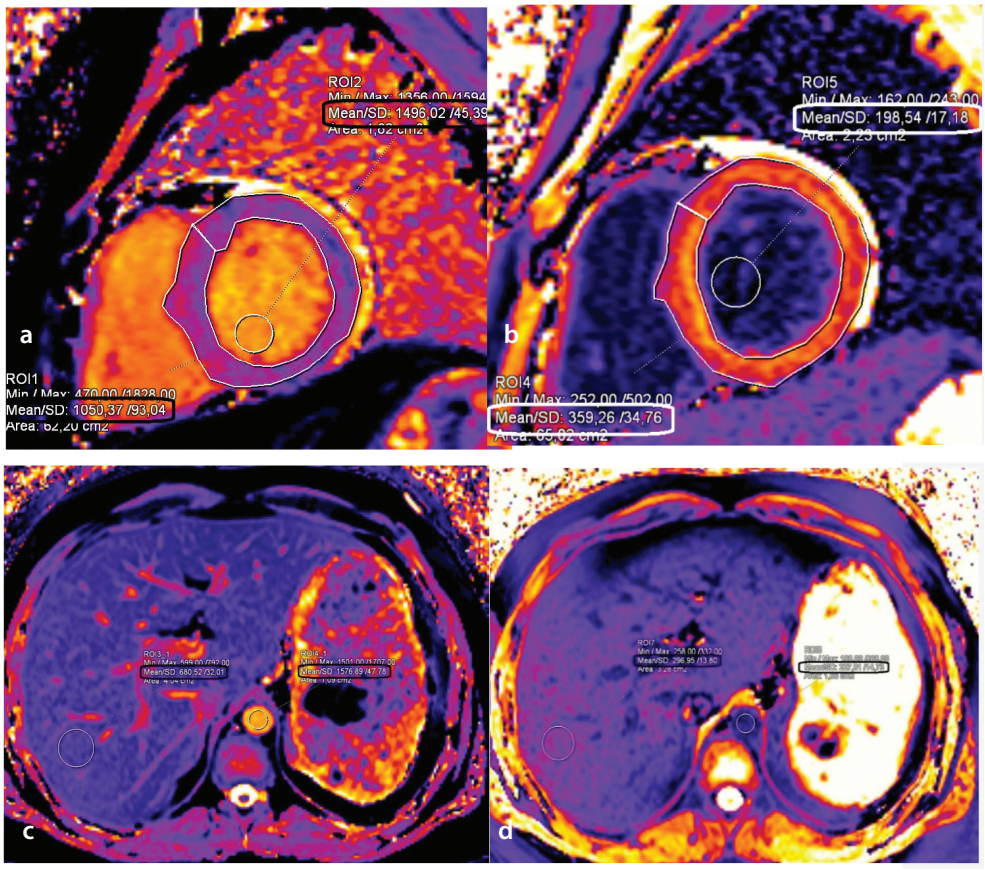


Figure 2. Measurement of native and post-contrast T1 values in myocardial and hepatic tissue for ECV assessment in a 25-year-old woman with SCA. (**a, b**) T1 relaxation times were measured from the myocardium and blood pool on **(a)** native and **(b)** post-contrast T1 map images obtained from short-axis views at the midventricular level. (**c, d**) T1 relaxation times were measured from the liver parenchyma and blood pool in the abdominal aorta on **(c)** native and **(d)** post-contrast T1 map images. ECV, extracellular volume; SCA, sickle cell anemia; SD, standard deviation; ROI, region of interest.

positioned to exclude the blood pool, endocardial border, trabeculations, and papillary muscles. In a 1.5-T magnetic field, myocardial T2* values are considered normal if they are greater than 20 ms.[8,13,14]

Hepatic T2* times were measured on hepatic T2* mapping images by placing a single, conservatively sized, circular-to-oval ROI in a homogeneous area of the right hepatic lobe on a representative slice, at least 1 cm from the liver capsule; regions containing large vessels or bile ducts, focal lesions, or susceptibility-related artifacts were visually excluded to minimize partial-volume effects (Figure 3). Based on hepatic T2* imaging values, hepatic iron overload is classified into four categories: normal (T2* > 6.3 ms), mild (T2*: 2.8–6.3 ms), moderate (T2*: 1.4–2.8 ms), and severe (T2* < 1.4 ms).[15,16]

Myocardial T2 times were calculated on T2 mapping images by drawing conservatively sized ROIs on the left ventricular myocardium at the mid-ventricular level. A global myocardial approach was used, with ROIs encompassing most of the left ventricular wall while excluding the blood pool, papillary muscles, and trabeculations to minimize partial-volume effects. Areas affected by susceptibility-related artifacts were visually identified and avoided during ROI placement.

TMF velocity–time curves were generated by placing an ROI at the center of the mitral valve orifice on phase images (Figure 4). Early (E) and late (A) diastolic filling waves were derived from these velocity–time curves. The E wave was defined as the peak early diastolic TMF velocity, and the A wave as the peak velocity during atrial contraction.

LA volumes were measured using the biplane area–length method. At the end of systole, the LA area and anteroposterior length were traced in four-chamber (A1–L1) and two-chamber (A2–L2) views. LA volume was calculated using the formula $0.85 \times A1 \times A2 / L$, where L represents the shorter of the

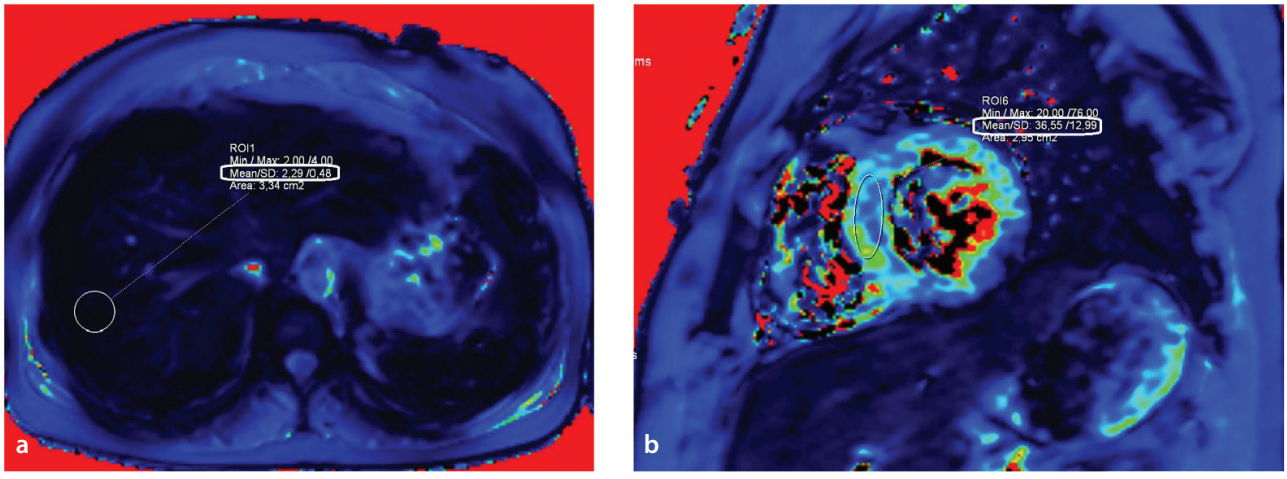


Figure 3. Measurement of hepatic and myocardial iron deposition in a 51-year-old man with SCA. **(a)** Hepatic T2* map image showing moderate iron deposition. **(b)** Cardiac T2* map image showing no iron deposition. SCA, sickle cell anemia; SD, standard deviation; ROI, region of interest.

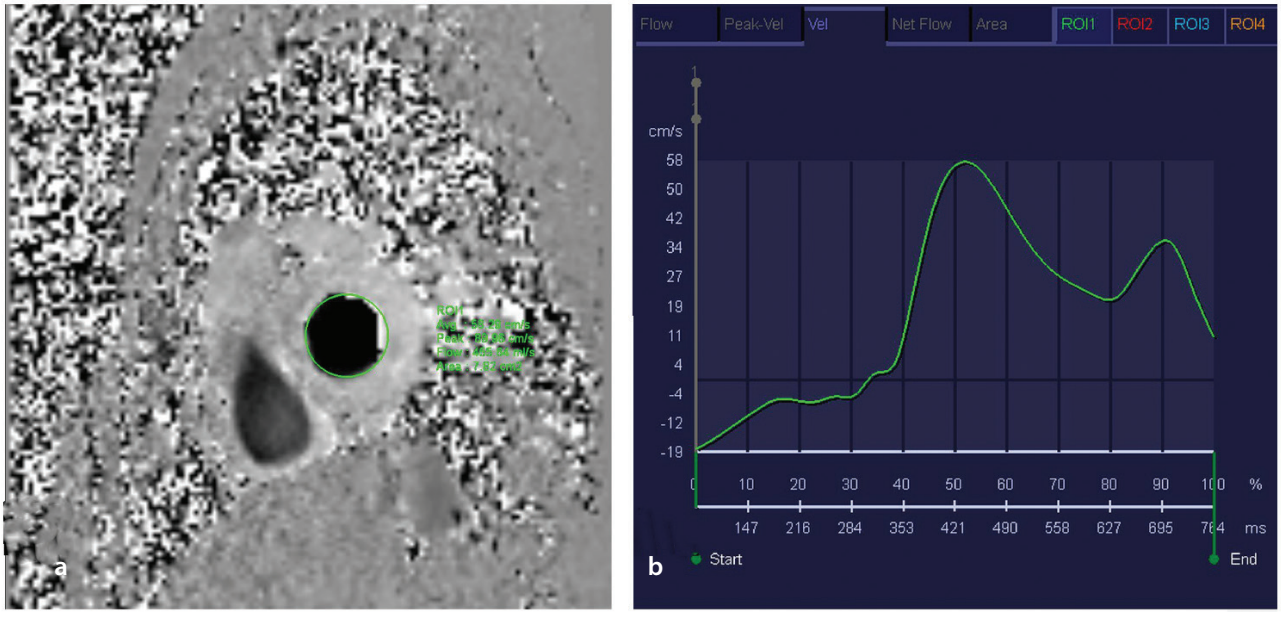


Figure 4. Obtaining the TMF curve in a healthy 30-year-old woman. Although the imaging plane was planned on the four-chamber cine view, the resulting through-plane PC-MRI acquisition corresponds anatomically to a short-axis orientation at the mitral valve level. **(a)** Through-plane PC-MRI phase image acquired with a VENC of 120 cm/s; a region of interest is placed within the mitral orifice to generate the TMF curve. **(b)** The resulting curve shows an E/A ratio of 1–2, consistent with normal filling. TMF, transmitral flow; PC-MRI, phase-contrast magnetic resonance imaging; VENC, velocity encoding.

two measured lengths (L1 or L2).[17] The LAVI was then calculated by indexing LA volume to body surface area and expressed as mL/m^2. Patients with an E/A ratio < 1 with normal or mildly increased LAVI were classified as having findings suggestive of an impaired relaxation filling pattern. Patients with an E/A ratio of 1–2 and increased LAVI were classified as having findings suggestive of a pseudonormal filling pattern. Patients with an E/A ratio > 2 with markedly increased LAVI were classified as having findings suggestive of a restrictive filling pattern (Figure 5).

Statistical analysis

Interobserver agreement was assessed using the intraclass correlation coefficient (ICC). Descriptive statistics for categorical variables were presented as frequencies and percentages, whereas continuous variables were expressed as mean ± standard deviation. The relationship between categorical variables was evaluated using the chi-square test. Variance equality between the patient and control groups was assessed using Levene's test, and, based on the results, the appropriate t-test (Student's or Welch's) was used to examine differences in mean measurements. In addition, one-sample t-tests were performed to compare the mean myocardial and hepatic ECV values of our patient cohort with previously published reference values. Pearson's correlation coefficient was used to assess the linear relationship between measurements. Statistical significance was defined as $P < 0.05$.

Results

Demographic and clinical characteristics

A total of 32 patients with SCA and 12 healthy individuals were included in the study. Demographic characteristics of the participants are presented in Table 1. There was no significant difference in mean age between the patient and control groups ($P = 0.083$). No participants in either group had a history of hypertension, diabetes mellitus, valvular heart disease, or known coronary artery disease. Among the patients, 27 were receiving hydroxyurea therapy, whereas 5 were not. Transfusion exposure was heterogeneous: 8 patients had no transfusion history. Of the 24 patients with a transfusion history, 13 received transfusions in the last year (range, 4–12 per year), whereas the remaining 11 had only sporadic transfusions in the past (typically 1–3 episodes) without a regular transfusion schedule. Among patients with a transfusion history, the interval between the most recent transfusion and MRI was at least 4 months in all cases. All MRI examinations were scheduled as outpatient scans and were performed during the steady-state period; none of the patients were imaged during an acute vaso-occlusive crisis.

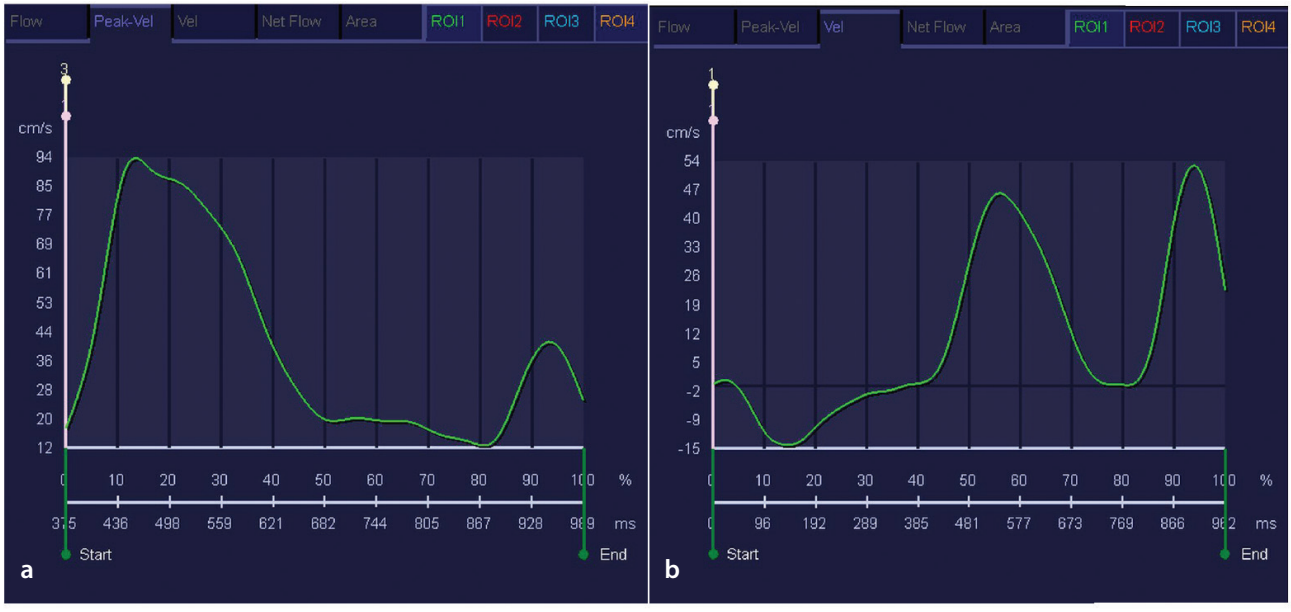


Figure 5. Transmitral flow curves showing impaired relaxation and restrictive filling patterns. **(a)** Transmitral flow pattern consistent with a restrictive filling pattern, showing an E/A ratio > 2 (E: 94, A: 39, E/A: 2.41) in a 27-year-old woman with SCA. **(b)** Transmitral flow pattern consistent with an impaired relaxation pattern, showing an E/A ratio < 1 (E: 47, A: 54, E/A: 0.8) in a 51-year-old man with SCA. SCA, sickle cell anemia; ROI, region of interest.

Table 1. Demographic characteristics of study participants

Characteristic	Control (n = 12)	Patients (n = 32)	*P* value
Age (years)	31.4 ± 6.8	37.5 ± 11.09	0.083
Male sex, n (%)	8 (66.7)	13 (40.6)	0.124
Hydroxyurea therapy, n (%)	NA	27 (84.4)	–
Transfusion (ever), n (%)	NA	24 (75)	–
Transfusions in the last year	NA	13 (40.6)	–
Hemoglobin (g/dL)	–	8.0 ± 1.3	–
Hematocrit (%)	–	24.8 ± 4.0	–

Values are presented as mean ± standard deviation. n, number; NA, not applicable.

Cardiac magnetic resonance imaging parameters

Cardiac MRI parameters are summarized in Table 2. Myocardial native T1 was significantly higher in patients with SCA than in controls (1,030.9 ± 28.4 ms in the SCA group vs. 1,000.3 ± 23.8 ms in controls; $P = 0.002$). In contrast, myocardial T2 values did not differ significantly between groups. Myocardial T2* values remained within the normal range in the SCA group, and no patient demonstrated myocardial iron accumulation. Cine-derived left ventricular end-diastolic volume index (LVEDVi), left ventricular end-systolic volume index (LVESVi), and left ventricular mass index were significantly higher in patients with SCA than in controls (all $P < 0.001$); LAVI was significantly higher in the SCA group than in controls (46.48 ± 15.35 vs. 30.58 ± 5.0 mL/m^2; $P < 0.001$); EF did not differ significantly between the two groups.

Myocardial extracellular volume findings

Myocardial ECV measurements are presented in Table 3. The mean myocardial ECV in the SCA group was 31.7%, which was higher than previously reported reference ranges.[18]

Within the SCA cohort, myocardial ECV was significantly higher in patients with findings suggestive of a restrictive filling pattern (n = 10) than in the remaining patients (n = 22) (34.14 ± 2.39% vs. 30.62 ± 2.67%; $P = 0.001$) (Table 4).

Distribution of diastolic dysfunction

DD was evaluated based on TMF-derived E/A ratios, assessed in conjunction with LAVI. In the SCA group, findings suggestive of DD were identified in 15 of 32 patients (46.9%), whereas none were observed in the control group (Table 2). The findings showed that 10 patients (31%) exhibited findings suggestive of a restrictive filling pattern, 2 (6%) showed findings suggestive of an impaired relaxation filling pattern, and 3 (9%) exhibited findings suggestive of a pseudonormal filling pattern; 17 patients (53%) had no findings suggestive of DD. The distribution of DD is shown in Figure 6. In a subgroup analysis, patients with TMF-derived E/A > 2 (n = 10) had significantly higher LAVI than the remaining patients (n = 22) (54.05 ± 10.12 vs. 43.0 ± 16.26 mL/m^2; $P = 0.027$) (Table 4).

Hepatic magnetic resonance imaging findings

Hepatic MRI parameters are summarized in Table 2. Hepatic iron accumulation was detected in 16 of 32 patients, and the mean hepatic T2* value was significantly lower in the SCA group than in controls ($P = 0.006$). Although the mean hepatic native T1 value was higher in the SCA group, the difference was not significant. In the SCA subgroup without hepatic iron deposition, the mean hepatic T1 value was significantly higher than in controls ($P < 0.001$).

The mean hepatic ECV was 46.1% in the entire SCA group and 40.4% in the subgroup without hepatic iron deposition, both higher than previously reported reference ranges.[19,20] Hepatic ECV measurements are presented in Table 3.

Interobserver agreement

Myocardial T1 relaxation times and ECV values were independently measured by two radiologists with 5 and 15 years of experience, respectively, whereas other parameters were assessed together. There was a high interobserver agreement for native T1 [ICC: 0.85, 95% confidence interval (CI): 0.80, 0.93] and ECV [ICC: 0.96 (95% CI: 0.93, 0.98)].

Table 2. Magnetic resonance imaging characteristics of study participants

Characteristic	Control (n = 12)	Patients (n = 32)	*P* value
Cardiac function parameters			
EF (%)	60 ± 4.1	60.7 ± 4.6	0.233
LAVI (mL/m^2)	30.58 ± 5	**46.48 ± 15.35**	**< 0.001**
LVEDVi (mL/m^2)	75.67 ± 12.95	**101.95 ± 16.75**	**< 0.001**
LVESVi (mL/m^2)	30.09 ± 6.50	**40.28 ± 9.28**	**< 0.001**
Left ventricular mass index (g/m^2)	54.49 ± 6.27	**76.95 ± 13.23**	**< 0.001**
Myocardial parameters			
Myocardial T1 (ms)	1,000.33 ± 23.76	**1,030.91 ± 28.40**	**0.002**
Myocardial T2 (ms)	47.92 ± 3.67	47.94 ± 3.16	0.985
Myocardial T2* (ms)	36.41 ± 5.24	39.25 ± 5.92	0.151
Hepatic parameters			
Hepatic T1 (ms)	537.83 ± 29.07	564.03 ± 108.88	0.402
Hepatic T1† (ms)	537.83 ± 29.07	**626.56 ± 61.45**	**< 0.001**
Hepatic T2* (ms)	19.15 ± 4.26	**12.20 ± 7.77**	**0.006**
Diastolic dysfunction			
DD present	0 (0%)	**15 (46.9%)**	–
DD absent	12 (100%)	**17 (53.1%)**	–

†: SCA subgroup without hepatic iron deposition (n = 16). Values are presented as mean ± standard deviation or n (%). Statistically significant measurements are shown in bold. EF, ejection fraction; LAVI, left atrial volume index; LVEDVi, left ventricular end-diastolic volume index; LVESVi, left ventricular end-systolic volume index; n, number; DD, diastolic dysfunction.

Table 3. Comparison of ECV values in the patient group and those in the literature

	Group	n	Mean	Standard deviation	*P* value
Myocardial ECV	Patient	32	**31.7%**	3.1	**< 0.001**
	Control*	81	25.3%	3.5	
Hepatic ECV†	Patient	16	**40.4%**	7.2	**< 0.001**
	Control**	22	25.9%	4.5	

*The control group in reference 18; **The control group in reference 19. †: SCA subgroup without hepatic iron deposition (n = 16). The *P* values were calculated using one-sample t-tests comparing the patient group's mean ECV values with published reference means. Statistically significant measurements are shown in bold. ECV, extracellular volume; n, number.

Table 4. Comparative evaluation of myocardial ECV and LAVI in patients with SCA with findings suggestive of a restrictive filling pattern versus the remaining SCA cohort

Parameter	Restrictive filling pattern group (n = 10)	Remaining SCA cohort (n = 22)	*P* value
Myocardial ECV (%)	34.14 ± 2.39	30.62 ± 2.67	0.001
LAVI (mL/m^2)	54.05 ± 10.12	43.03 ± 16.26	0.027

Values are presented as mean ± standard deviation. ECV, extracellular volume; LAVI, left atrial volume index; SCA, sickle cell anemia; n, number.

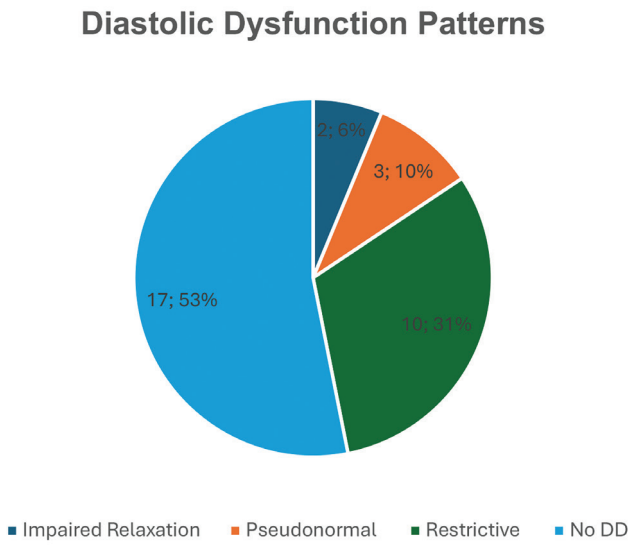


Figure 6. Distribution of diastolic filling patterns in the patient group (n = 32) based on TMF-derived E/A ratio in conjunction with LAVI. Values are shown as n (%). TMF, transmitral flow; LAVI, left atrial volume index; DD, diastolic dysfunction.

Discussion

The present study was designed to evaluate myocardial fibrosis in patients with SCA using advanced MRI tissue mapping techniques and ECV quantification, and to assess associated DD through TMF analysis and LA volume measurements. Hepatic fibrosis-related MRI metrics were also evaluated. The principal findings of this study demonstrated that patients with SCA exhibited significantly increased myocardial native T1 and ECV values, suggesting expansion of the myocardial extracellular space, largely consistent with diffuse interstitial fibrosis in this cohort, in the absence of myocardial iron overload as indicated by normal myocardial T2* values. Importantly, diastolic function assessment revealed a high prevalence of findings suggestive of advanced DD, including restrictive filling patterns, in relatively young patients. Notably, myocardial ECV was significantly higher in patients with findings suggestive of a restrictive filling pattern than in the remaining SCA cohort, supporting an association between diffuse myocardial fibrosis and advanced diastolic filling abnormalities in SCA. In a secondary, exploratory analysis, hepatic tissue characterization demonstrated elevated native T1 and ECV values, particularly in patients without hepatic iron deposition, supporting fibrosis-related tissue remodeling beyond iron-related effects.

The increase in native T1 values, reflecting tissue differences, particularly in conditions involving fibrosis and edema, along with the increase in ECV values, which correlate strongly with tissue collagen content, suggests myocardial fibrosis in patients with SCA. Cardiomyopathy, the leading cause of mortality in SCA, is associated with cardiac chamber enlargement, perfusion abnormalities, myocardial fibrosis, DD, and, occasionally, iron deposition.[21] In a study by Bakeer et al.[22] using cardiac imaging–histopathology correlation in mice with SCA, it was determined that, in addition to anemia-induced hyperdynamic physiology, a restrictive condition was also present, which was associated with myocardial fibrosis. In another study, Alsaied et al.[23] identified the relationship between LA dysfunction and myocardial fibrosis in patients with SCA. Furthermore, Niss et al.[24] found that sickle cell-related cardiomyopathy was associated with hyperdynamic processes and DD, with DD being linked to myocardial fibrosis. In that study, significantly elevated T1 relaxation times and ECV values were observed in the patient group, consistent with our results. When acquisition and post-processing are standardized, ECV measurements show good reproducibility; moreover, the dependence of ECV on field strength and sequence choice appears lower than for native T1.[7,25] Moreover, there is a strong correlation between ECV and histopathologically measured collagen levels in fibrosis.[26] This makes ECV a useful tool for identifying myocardial fibrosis and a promising, non-invasive alternative to labor-intensive procedures. However, ECV reflects expansion of the myocardial extracellular space and is not entirely specific for fibrosis; it may also be elevated in the presence of myocardial edema/inflammation or infiltrative cardiomyopathies. In our cohort, infiltrative disease was considered unlikely given the young age and clinical context, and myocardial T2 values were not increased compared with

controls, arguing against clinically relevant myocardial edema at the time of imaging. Taken together, elevated native T1/ECV in the presence of normal T2 supports diffuse interstitial fibrosis as the likely predominant explanation, although subtle edema cannot be completely excluded.

Studies have shown a significant link between collagen content, ventricular relaxation, and diastolic function. In experimental models, reducing myocardial collagen with bacterial collagenase[27] or plasmin[28] increased sarcomere length and ventricular volume, whereas fibrotic conditions with higher collagen levels impaired elasticity and diastolic function. These findings suggest that myocardial fibrosis, characterized by increased collagen content, could be biochemically linked to DD in patients with SCA. Both Niss et al.[24] and Alsaied et al.[23] evaluated cardiac functions using transthoracic echocardiography (TTE). Alsaied et al.[23] identified an association between myocardial fibrosis and LA dysfunction. Similarly, Niss et al.[24] proposed a connection between myocardial fibrosis and DD. In our study, we assessed diastolic function using TMF indices derived from PC-CMR. Comparative studies have shown that these PC-CMR–derived indices correlate well with Doppler TTE, with good agreement particularly for the E/A ratio and deceleration time when standardized acquisition and analysis are applied.[29-31] Nevertheless, invasive hemodynamic assessment (e.g., right heart catheterization with pulmonary capillary wedge pressure) remains the reference standard for confirming elevated filling pressures;[32] therefore, PC-CMR–derived diastolic indices warrant further validation against invasive metrics in larger cohorts.

A substantial prevalence of findings suggestive of a restrictive filling pattern was observed in relatively young patients with SCA, representing another key finding of this study. To the best of our knowledge, this is the first study to evaluate diastolic function in patients with SCA using MRI based on LA volume measurements and TMF curves. Among the 32 patients, 15 had findings suggestive of DD: 2 with findings suggestive of impaired relaxation filling pattern (E/A ratio < 1, aged 51 and 53 years), 3 with findings suggestive of pseudonormal filling pattern (E/A ratio 1–2, significantly increased LAVI, aged 60, 51, and 51 years), and 10 with findings suggestive of a restrictive filling pattern (E/A ratio > 2, mean age: 33.3 years). This raises the possibility that aging may also play a role in the etiology of impaired relaxation and pseudonormal filling patterns, suggesting that age-related changes may influence these measurements. Indeed, the DD that emerged in these 5 patients with SCA, who had no comorbidities such as diabetes or hypertension and no known history of cardiac disease, may be related to myocardial fibrosis associated with SCA. However, it would not be accurate to ignore age-related changes. A particularly striking finding was that 10 relatively young patients (mean age: 33.3 years), all without comorbidities other than SCA, showed TMF and LAVI findings suggestive of a restrictive filling pattern. In these patients, the E/A ratio was >2, along with a markedly increased LAVI (54.05 ± 10.12 mL/m^2), and all had elevated ECV values (minimum 28.7%, maximum 36.8%). The underlying pathology in a restrictive filling pattern is myocardial stiffening and decreased elasticity. We believe that the diffuse myocardial fibrosis observed in SCA is associated with this pathology. Consistent with this interpretation, myocardial ECV was significantly higher in patients with findings suggestive of a restrictive filling pattern than in the remaining SCA cohort ($P = 0.001$) (Table 4), suggesting an association between diffuse interstitial fibrosis and advanced DD patterns. Due to the cross-sectional design, temporal or causal relationships between fibrosis-related MRI findings and diastolic abnormalities cannot be established; therefore, these observations should be interpreted as hypothesis-generating. From a methodological perspective, our diastolic evaluation relied on PC-CMR–derived TMF (E/A) and LAVI and did not incorporate additional diastolic parameters, such as tissue Doppler e' and E/e', pulmonary venous flow, tricuspid regurgitation velocity, or invasive filling pressures. In SCA, chronic anemia and a high-output state may influence TMF and contribute to a restrictive-like pattern; therefore, this pattern should be interpreted in the clinical context and not equated with a clinical diagnosis of heart failure with preserved EF or restrictive cardiomyopathy. Consistent with a chronic volume-loaded, high-output physiology, LVEDVi, LVESVi, and left ventricular mass index were higher in patients with SCA ($P < 0.001$), supporting volume load-related structural remodeling, whereas EF remained similar between groups, indicating preserved systolic function.

Using T2* mapping, we observed no cardiac iron accumulation in patients with SCA, consistent with the literature. Previous studies have likewise shown that cardiac iron is uncommon in SCA despite frequent hepatic iron overload. For example, Junqueira et al.[33] reported hepatic iron accumulation in 26/30 patients with only one case of cardiac iron, and Inati et al.[34] found no cardiac iron in 20 patients with SCA. In line with prior reports, hepatic iron accumulation was present in a substantial proportion of our cohort. Hepatic fibrosis may develop due to both iron accumulation and the disease's pathophysiology. ECV measurements, which are valuable in evaluating myocardial fibrosis, may also be useful in assessing hepatic fibrosis. Mesropyan et al.[19] conducted a study involving 68 patients with cirrhosis and 22 healthy individuals, measuring hepatic ECV and finding that ECV was higher in the patients with cirrhosis than in the control group. Following this approach, we, to the best of our knowledge, measured hepatic parenchymal ECV values in patients with SCA for the first time. However, hepatic iron deposition can shorten native T1, thereby masking underlying fibrosis. Iron-corrected T1 (cT1) accounts for this effect by incorporating an iron-sensitive measure, such as T2* or R2*, thereby improving the interpretation of T1 in the presence of iron. Accordingly, cT1 may provide a more reliable assessment of fibro-inflammatory changes in iron-loaded livers than native T1 alone. Because cT1 was not available in our study due to software limitations, we analyzed hepatic T1/ECV measurements separately in patients with and without hepatic iron accumulation.

In patients without hepatic iron deposition, hepatic native T1 and ECV values were significantly higher than in controls, consistent with fibrotic remodeling related to recurrent vaso-occlusions and resultant ischemia in SCA, even in the absence of significant iron accumulation. Additionally, iron deposition clearly contributes to fibrosis at the biochemical level.[35] When including patients with hepatic iron accumulation in the analysis of the entire patient group, hepatic native T1 values were higher than those of the control group but did not reach statistical significance, likely because iron deposition lowers T1 values. Similarly, hepatic ECV values for the entire patient group were markedly higher than the ranges reported in the literature and the values observed in patients without iron accumulation. However, it remains unclear whether this increase is solely due to the contribution of iron deposition to fibrosis. This issue requires further investigation using a larger patient cohort and studies that employ cT1 values to provide clarity. Nonetheless, hepatic native T1/ECV are useful surrogates but are not specific for fibrosis. Liver MOLLI/shMOLLI T1 measurements can

be influenced by hepatic fat (via fat–water/off-resonance effects, which may cause an apparent T1 overestimation in steatosis) and by diffuse inflammatory/congestive changes, whereas iron has a more pronounced T1-shortening confounding effect.[36,37] Accordingly, although we addressed iron via subgroup analyses, residual confounding from unmeasured steatosis or other diffuse hepatic processes cannot be completely excluded. Future studies incorporating quantitative fat assessment [proton density fat fraction (PDFF)] may further reduce confounding and strengthen the interpretation of hepatic fibrosis-related MRI metrics.

Our study has several limitations. First, this was a relatively small observational study, which limits the generalizability of our findings. Additionally, this was a single-center, adult-predominant cohort with high hydroxyurea use and specific transfusion patterns; therefore, our findings may not be generalizable to pediatric populations with SCA, patients managed with different treatment strategies, or regions with differing disease severity. Subgroup analyses were small—particularly DD subgroups and hepatic ECV subgroups based on iron status—limiting the robustness of subgroup comparisons and increasing the risk of sampling variability in subgroup classification. Moreover, no formal correction for multiple comparisons was applied despite multiple subgroup analyses, t-tests against literature reference values, and correlation analyses; therefore, the findings should be interpreted with caution. Although we observed clear differences in key MRI metrics, conclusions regarding associations between tissue characterization findings and DD should be interpreted as hypothesis-generating. Second, although major comorbidities were absent by study design, we could not comprehensively account for potential confounders, including age-related effects, disease severity, and treatment exposure (e.g., transfusion history and hydroxyurea therapy). Although treatment histories were available, the sample size and study design did not allow a reliable assessment of their impact on diastolic indices or MRI-based tissue metrics; therefore, residual confounding cannot be ruled out. Additionally, detailed clinical data and comprehensive laboratory parameters—including liver function tests and cardiac biomarkers—were not available, which could have provided valuable correlations with imaging findings. Third, we could not administer contrast to controls for ethical reasons; as such, control ECV values were not available, and patient ECV measurements were compared with literature reference ranges. This comparison is subject to methodological variability across T1-mapping/ECV techniques and platforms, meaning our ECV findings should be interpreted cautiously. Published reference ranges were used primarily for context, and these comparisons should not be interpreted as definitive abnormality thresholds. Fourth, hepatic tissue characterization was limited by the inability to use cT1 due to a lack of appropriate software, and hepatic steatosis was not quantitatively assessed (e.g., by PDFF), which may affect the specificity of hepatic native T1/ECV for fibrosis. In addition, hepatic fibrosis was not confirmed by liver biopsy, meaning hepatic findings should be considered exploratory and are not equivalent to histologic fibrosis staging. Fifth, echocardiographic parameters (e.g., E/e' and echo-derived E/A) were not available for most participants, precluding a systematic echo–CMR correlation analysis. As such, the CMR-based DD classification should be interpreted as suggestive, and future studies using standardized echocardiography and/or invasive hemodynamic reference measurements would be valuable. Finally, the absence of findings suggestive of DD in the control group should be interpreted cautiously, given the small control sample size (n = 12) and the lack of universally established normal reference ranges and diagnostic thresholds for PC-CMR–derived diastolic indices such as the E/A ratio. Future studies with larger sample sizes, more balanced DD subgroups, multivariable adjustment for confounders, the use of cT1 values, and ethically feasible inclusion of control ECV measurements are needed to confirm and extend these findings.

In conclusion, in patients with SCA, myocardial T1 and ECV values were significantly higher, suggesting expansion of the myocardial extracellular space, largely consistent with diffuse interstitial fibrosis in the studied clinical context. Moreover, T2* mapping revealed no cardiac iron deposition, indicating that cardiac findings were unlikely to be related to myocardial iron accumulation. Furthermore, TMF curves and LA volume measurements revealed findings suggestive of a restrictive filling pattern in a considerable number of young patients without any comorbidities other than SCA, and myocardial ECV was significantly higher in these patients, supporting an association between diffuse interstitial fibrosis and advanced filling patterns. These data suggest that CMR, which allows non-invasive and comprehensive evaluation of myocardial tissue characteristics and cardiac function in patients with SCA, may have clinical value for early diagnosis and follow-up. In liver evaluations using T2* mapping, iron accumulation was detected in some patients, whereas in the group without iron deposition, significantly increased hepatic T1 and ECV values were observed. These secondary hepatic findings should be interpreted as exploratory and hypothesis-generating, and suggest that combined liver T2* and T1/ECV mapping may provide complementary information on iron burden and tissue remodeling in SCA, pending validation in larger studies. Further studies with dedicated liver endpoints are needed to clarify the clinical implications of these observations.

Footnotes

Conflict of interest disclosure

The authors declared no conflicts of interest.

Funding

This study was supported by the Scientific Research Projects Unit of Mersin University (Project No: 2022-2-TP3-4766).

References

1. Rees DC, Williams TN, Gladwin MT. Sickle-cell disease. *Lancet*. 2010;376(9757):2018-2031. [Crossref]
2. Fitzhugh CD, Lauder N, Jonassaint JC, et al. Cardiopulmonary complications leading to premature deaths in adult patients with sickle cell disease. *Am J Hematol*. 2010;85(1):36-40. [Crossref]
3. Sachdev V, Machado RF, Shizukuda Y, et al. Diastolic dysfunction is an independent risk factor for death in patients with sickle cell disease. *J Am Coll Cardiol*. 2007;49:472-479. [Crossref]
4. Manganas K, Delicou S, Xydaki A, et al. Predisposing factors for advanced liver fibrosis in patients with sickle cell disease. *Br J Haematol*. 2023;202(6):1192-1198. [Crossref]
5. American College of Cardiology Foundation Task Force on Expert Consensus Documents; Hundley WG, Bluemke DA, et al. ACCF/ACR/AHA/NASCI/SCMR 2010 expert consensus document on cardiovascular magnetic resonance: a report of the American College of Cardiology Foundation Task Force on Expert Consensus Documents. *J Am Coll Cardiol*. 2010;55(23):2614-2662. [Crossref]
6. Prasad SK, Akbari T, Bishop MJ, Halliday BP, Leyva-Leon F, Marchlinski F. Late gadolinium enhancement imaging and sudden cardiac death. *Eur Heart J*. 2025;46(36):3555-3568. [Crossref]

7. Messroghli DR, Moon JC, Ferreira VM, et al. Clinical recommendations for cardiovascular magnetic resonance mapping of T1, T2, T2* and extracellular volume: a consensus statement by the Society for Cardiovascular Magnetic Resonance (SCMR) endorsed by the European Association for Cardiovascular Imaging (EACVI). *J Cardiovasc Magn Reson*. 2017;19(1):75. Erratum in: *J Cardiovasc Magn Reson*. 2018;20(1):9. [Crossref]
8. Triadyaksa P, Oudkerk M, Sijens PE. Cardiac T2* mapping: techniques and clinical applications. *J Magn Reson Imaging*. 2020;52(5):1340-1351. [Crossref]
9. Tipirneni-Sajja A, Shrestha U, Esparza J, et al. State-of-the-art quantification of liver iron with MRI-vendor implementation and available tools. *J Magn Reson Imaging*. 2025;61(3):1110-1132. [Crossref]
10. Obmann VC, Ardoino M, Klaus J, et al. MRI extracellular volume fraction in liver fibrosis: a comparison of different time points and blood pool measurements. *J Magn Reson Imaging*. 2024;60(4):1678-1688. [Crossref]
11. Torlasco C, Cassinerio E, Roghi A, et al. Role of T1 mapping as a complementary tool to T2* for non-invasive cardiac iron overload assessment. *PLoS One*. 2018;13(2):e0192890. [Crossref]
12. Alam MH, Auger D, Smith GC, et al. T1 at 1.5T and 3T compared with conventional T2* at 1.5T for cardiac siderosis. *J Cardiovasc Magn Reson*. 2015;17:102. [Crossref]
13. Koohi F, Kazemi T, Miri-Moghaddam E. Cardiac complications and iron overload in beta thalassemia major patients-a systematic review and meta-analysis. *Ann Hematol*. 2019;98(6):1323-1331. [Crossref]
14. Kawel-Boehm N, Maceira A, Valsangiacomo-Buechel ER, et al. Normal values for cardiovascular magnetic resonance in adults and children. *J Cardiovasc Magn Reson*. 2015;17(1):29. [Crossref]
15. Labranche R, Gilbert G, Cerny M, et al. Liver iron quantification with MR imaging: a primer for Radiologists. *Radiographics*. 2018;38(2):392-412. [Crossref]
16. Khadivi Heris H, Nejati B, Rezazadeh K, et al. Evaluation of iron overload by cardiac and liver T2* in β-thalassemia: correlation with serum ferritin, heart function and liver enzymes. *J Cardiovasc Thorac Res*. 2021;13(1):54-60. [Crossref]
17. Caudron J, Fares J, Bauer F, Dacher JN. Evaluation of left ventricular diastolic function with cardiac MR imaging. *Radiographics*. 2011;31:239-259. [Crossref]
18. Sado DM, Flett AS, Banypersad SM, et al. Cardiovascular magnetic resonance measurement of myocardial extracellular volume in health and disease. *Heart*. 2012;98(19):1436-1441. [Crossref]
19. Mesropyan N, Kupczyk PA, Dold L, et al. Assessment of liver cirrhosis severity with extracellular volume fraction MRI. *Sci Rep*. 2022;12(1):9422. [Crossref]
20. Dolan RS, Stillman AE, Davarpanah AH. Feasibility of hepatic T1-mapping and extracellular volume quantification on routine cardiac magnetic resonance imaging in patients with infiltrative and systemic disorders. *Acad Radiol*. 2022;29(Suppl 4):S100-S109. [Crossref]
21. Desai AA, Patel AR, Ahmad H, et al. Mechanistic insights and characterization of sickle cell disease-associated cardiomyopathy. *Circ Cardiovasc Imaging*. 2014;7(3):430-437. [Crossref]
22. Bakeer N, James J, Roy S, et al. Sickle cell anemia mice develop a unique cardiomyopathy with restrictive physiology. *Proc Natl Acad Sci U S A*. 2016;113(35):E5182-E5191. [Crossref]
23. Alsaied T, Niss O, Tretter JT, et al. Left atrial dysfunction in sickle cell anemia is associated with diffuse myocardial fibrosis, increased right ventricular pressure and reduced exercise capacity. *Sci Rep*. 2020;10:1767. Erratum in: *Sci Rep*. 2020;10(1):4880. [Crossref]
24. Niss O, Fleck R, Makue F, et al. Association between diffuse myocardial fibrosis and diastolic dysfunction in sickle cell anemia. *Blood*. 2017;130(2):205-213. [Crossref]
25. Moon JC, Messroghli DR, Kellman P, et al. Myocardial T1 mapping and extracellular volume quantification: a Society for Cardiovascular Magnetic Resonance (SCMR) and CMR Working Group of the European Society of Cardiology consensus statement. *J Cardiovasc Magn Reson*. 2013;15:92. [Crossref]
26. Sibley CT, Noureldin RA, Gai N, et al. T1 mapping in cardiomyopathy at cardiac MR: comparison with endomyocardial biopsy. *Radiology*. 2012;265:724-732. [Crossref]
27. MacKenna DA, Omens JH, McCulloch AD, Covell JW. Contribution of collagen matrix to passive left ventricular mechanics in isolated rat hearts. *Am J Physiol*. 1994;266:H1007-H1018. [Crossref]
28. Stroud JD, Baicu CF, Barnes MA, Spinale FG, Zile MR. Viscoelastic properties of pressure overload hypertrophied myocardium: effect of serine protease treatment. *Am J Physiol Heart Circ Physiol*. 2002;282:H2324-H2335. [Crossref]
29. Rathi VK, Doyle M, Yamrozik J, et al. Routine evaluation of left ventricular diastolic function by cardiovascular magnetic resonance: a practical approach. *J Cardiovasc Magn Reson*. 2008;10(1):36. [Crossref]
30. Bollache E, Redheuil A, Defrance C, et al. The clinical value of phase-contrast CMR mitral inflow diastolic parameters: comparison with echocardiography. *J Cardiovasc Magn Reson*. 2011;13(Suppl 1):P32. [Crossref]
31. Fujikura K, Sathya B, Acharya T, et al. CMR provides comparable measurements of diastolic function as echocardiography. *Sci Rep*. 2024;14(1):11658. [Crossref]
32. Nagueh SF, Sanborn DY, Oh JK, et al. Recommendations for the evaluation of left ventricular diastolic function by echocardiography and for heart failure with preserved ejection fraction diagnosis: an update from the American Society of Echocardiography. *J Am Soc Echocardiogr*. 2025;38(7):537-569. [Crossref]
33. Junqueira FP, Fernandes JL, Cunha GM, et al. Right and left ventricular function and myocardial scarring in adult patients with sickle cell disease: a comprehensive magnetic resonance assessment of hepatic and myocardial iron overload. *J Cardiovasc Magn Reson*. 2013;15(1):83. [Crossref]
34. Inati A, Musallam KM, Wood JC, Sheikh-Taha M, Daou L, Taher AT. Absence of cardiac siderosis by MRI T2* despite transfusion burden, hepatic and serum iron overload in Lebanese patients with sickle cell disease. *Eur J Haematol*. 2009;83:565-571. [Crossref]
35. Mehta KJ, Farnaud SJ, Sharp PA. Iron and liver fibrosis: mechanistic and clinical aspects. *World J Gastroenterol*. 2019;25:521-538. [Crossref]
36. Mozes FE, Tunnicliffe EM, Moolla A, et al. Mapping tissue water T1 in the liver using the MOLLI T1 method in the presence of fat, iron and B0 inhomogeneity. *NMR Biomed*. 2019;32:e4030. [Crossref]
37. Thomaides-Brears HB, Lepe R, Banerjee R, Duncker C. Multiparametric MR mapping in clinical decision-making for diffuse liver disease. *Abdom Radiol (NY)*. 2020;45:3508-3522. [Crossref]